

Online verification and management scheme of gateway meter flow in the power system by machine learning

Chong Li ^{Corresp., 1}, hao Wang ¹, Hongtao Shen ¹, Peng Yang ², Yi Wang ¹, Qian li ¹, Chuan Li ¹, Bing Li ¹, Rongkun Guo ¹, Ruiming Wang ¹

¹ State Grid Hebei Marketing Service Center, Shijiazhuang, HeBei, China

² State Grid Hebei electric power company, Shijiazhuang, HeBei, China

Corresponding Author: Chong Li

Email address: chunglee3181@126.com

At present, in the process of calibrating electric energy meters, manual meter reading and dismantling inspection or regular sampling inspection by professionals are often used. To improve the work efficiency and verification accuracy, this research integrates machine learning (ML) into the scheme of online verification and management of gateway meter flow in the power system. First, the Faster-Region Convolutional Neural Network (Faster-RCNN) model and the Single Shot MultiBox Detector (SSD) model are applied to the recognition system of dial readings. Then, the collected measurement data is preprocessed, and it is excluded under light load conditions. Next, the estimation error model and the solution equation of the electricity meter are established based on the preprocessed data. The operation error of the electricity meter is estimated and the estimation accuracy is checked by the limited memory recursive least squares algorithm (LMRLSA). Finally, combined with the remote verification results, the business assistant decision-making is carried out. A total of 528 images of meter readings are selected to test the proposed dial reading recognition system, and the accuracy of the test is 98.49%. In addition, the influence of various parameters on the error results of the electricity meter is also explored. The results demonstrate that when the memory length ranges from 600 to 1200 and the line loss error is less than 5%, the accuracy of the electricity meter error estimation is the most suitable. Meanwhile, to avoid over-checking, the measurement data at light load should be removed as much as possible. Experiments manifest that the proposed algorithm can properly eliminate the influence of old measurement data on the error parameter estimation, and improve the accuracy of the error parameter estimation value. The memory length is adjusted to ensure the real-time performance of the electricity meter error estimation, and realize the function of online monitoring. This research has certain reference significance for realizing the online verification and management of gateway meter flow in the power system.

Online Verification and Management Scheme of Gateway Meter Flow in the Power System by Machine Learning

Chong Li ^{1*}, Hao Wang¹, Hongtao Shen¹, Peng Yang², Yi Wang¹, Qian li¹, Chuan Li¹, Bing Li¹, Rongkun Guo¹, Ruiming Wang¹

1. State Grid Hebei Marketing Service Center; HeBei Shijiazhuang; 050000; China

2. State Grid Hebei electric power company; HeBei Shijiazhuang; 050000; China

**Corresponding author: Chong Li, chunglee3181@126.com*

Abstract: At present, in the process of calibrating electric energy meters, manual meter reading and dismantling inspection or regular sampling inspection by professionals are often used. To improve the work efficiency and verification accuracy, this research integrates machine learning (ML) into the scheme of online verification and management of gateway meter flow in the power system. First, the Faster-Region Convolutional Neural Network (Faster-RCNN) model and the Single Shot MultiBox Detector (SSD) model are applied to the recognition system of dial readings. Then, the collected measurement data is preprocessed, and it is excluded under light load conditions. Next, the estimation error model and the solution equation of the electricity meter are established based on the preprocessed data. The operation error of the electricity meter is estimated and the estimation accuracy is checked by the limited memory recursive least squares algorithm (LMRLSA). Finally, combined with the remote verification results, the business assistant decision-making is carried out. A total of 528 images of meter readings are selected to test the proposed dial reading recognition system, and the accuracy of the test is 98.49%. In addition, the influence of various parameters on the error results of the electricity meter is also explored. The results demonstrate that when the memory length ranges from 600 to 1200 and the line loss error is less than 5%, the accuracy of the electricity meter error estimation is the most suitable. Meanwhile, to avoid over-checking, the measurement data at light load should be removed as much as possible. Experiments manifest that the proposed algorithm can properly eliminate the influence of old measurement data on the error parameter estimation, and improve the accuracy of the error parameter estimation value. The memory length is adjusted to ensure the real-time performance of the electricity meter error estimation, and realize the function of online monitoring. This research has certain reference significance for realizing the online verification and management of gateway meter flow in the power system.

Keywords: Machine learning; Faster-RCNN model; SSD model; Limited memory recursive least squares algorithm; Dial reading identification; Online verification; Line loss; Light load condition

1. Introduction

At present, the main way for power companies to verify the accuracy of the gateway meter flow of the power system (hereinafter referred to as the total meter) is to carry out dismantling inspection or regularly carry instruments and equipment to the site for periodic sampling inspection by professionals [1]. With the expansion of the power grid, China has more than 500 million meters in operation. The existing verification mode has high work intensity, a long verification period and low management efficiency, and it is difficult to meet the requirements of condition maintenance and replacement of smart meters [2]. To realize the transformation of smart meters from regular verification to state verification and ensure the accuracy of measurement, it is imperative to explore an efficient and accurate online remote verification and management solution for the operation of the total meter.

The existing online remote verification methods for smart meters based on measurement data analysis mainly include ordinary least squares inversion and weighted recursive least squares. However, the solution accuracy and practicability of the method are not high, and it is easily affected by factors such as the user's power consumption level, the number of user meters, and data quality [3]. Wang et al. (2020) proposed the idea of the error analysis of the electricity meters based on advanced meter infrastructure (AMI) measurement data, without using external standard instruments, only by comparing the existing meters in the cluster to calculate the error [4]. However, this method fails to consider the influence of the algorithm such as the number of measurement periods, the number of meters in the station area, and the out-of-tolerance of a single low-voltage user meter on the model results. The Marketing Department of State Grid Corporation of China has carried out research on the state inspection plan of the electricity

53 meters. Through four triggering methods: family defects, online monitoring, on-site inspection, and regular triggering,
54 the operation state of the electricity meters is scored, and corresponding inspection strategies are generated according
55 to the scoring results [5]. The relevant research results qualitatively divide the electricity meter into several states, and
56 the analysis results are relatively rough, and it is impossible to realize the remote accurate verification of the electricity
57 meter.

58 To simplify the verification method of the total meter and improve the verification accuracy, an online
59 verification and management scheme of gateway meter flow in the power system by machine learning (ML) is
60 proposed. Firstly, the automatic meter reading is realized through the scheme of the dial reading recognition system
61 of the Faster-Region Convolutional Neural Networks (Faster-RCNN) model and the Single Shot MultiBox Detector
62 (SSD) model. Secondly, the automatic meter reading data is used to estimate the operation error of the electricity
63 meter based on the limited memory recursive least squares algorithm (LMRLSA). The error estimation results of the
64 electric meter are verified and analyzed, and the online remote verification results of the electric meter are combined
65 to make business decision-making. Finally, the system is verified and tested, which proves that the proposed scheme
66 is scientific and feasible. The research has certain reference significance for realizing remote intelligent online meter
67 reading and verification management of the electricity meter.

68

69 2. Design of the Scheme

70

71 2.1 Faster-RCNN model and SSD model

72

73 The Faster-RCNN model was proposed in 2015. The main feature of this model is that the model is large in size
74 and has a strong ability to extract features. Therefore, the Faster-RCNN model is used to identify the specific readings
75 of the dial image, but its running speed is relatively slow [6]. The network structure of the model is shown in Figure
76 1:

77

Figure 1 The network structure of the Faster-RCNN model

78

79 First, when a picture is input, and the picture is adjusted to a fixed size. Then, the feature map is obtained by
80 processing the convolutional neural network (CNN). Next, the candidate box is generated by the Region Proposal
81 Networks (RPN), and the candidate box and feature map generated by the RPN are input into the Regions of interest
82 (ROI) pooling layer to obtain a fixed-size proposal feature map. Finally, the candidate box is classified and regressed
83 through the fully connected layer to obtain a more accurate target frame [7,8].

84

85 The SSD model is characterized by relatively small size, high accuracy in detecting large targets, and the
86 advantage of fast detection [9]. Therefore, the SSD model is adopted to detect the effective reading area of the dial
87 image. The core of the SSD model is to predict the category score and offset of the candidate box. Simultaneously,
88 candidate boxes of different sizes can be obtained by predicting on feature maps of different scales [10]. The network
89 structure of the SSD model is shown in Figure 2:

90

Figure 2 The network structure of the SSD model

91

92 The SSD model is different from the Faster-RCNN model in object detection. The Faster-RCNN model first
93 generates candidate regions through RPN, then classifies these candidate regions and calculates location information
94 through regression. However, the SSD model obtains a series of candidate regions on the feature maps of different
95 scales, and each point on the feature maps of different scales corresponds to different positions of the original image,
96 so high-precision detection results can be obtained [11, 12].

97

98 2.2 Realization of image recognition function

99

100 In this research, model training is done on Google's open-source TensorFlow framework. As an excellent
101 development framework for ML, TensorFlow provides developers with a large number of mature model
102 implementation solutions. For object detection tasks, TensorFlow provides the TensorFlow Object Detection API
103 open-source framework in its models' subproject. This framework has been widely used in Google's computer vision
104 applications. An open-source framework is adopted, which can easily build, train, and deploy object detection models
105 [13-15]. In the electricity meter reading recognition, two models are mainly trained, the first is the SSD model trained
106 to detect the effective reading area of the electricity meter screen, and the second is the Faster-RCNN model trained
107 to identify the readings in the effective reading area. The specific training process of the SSD model is shown in Figure
108 3:

109

Figure 3 The specific training process of the SSD model

110

When training the SSD model, first, the input meter image is resized, the height of the image is uniformly set to

109 500px, and the width is scaled proportionally. Then, LabelImg software is used to label the effective reading area of
 110 the image screen, a training sample set is constructed, and an XML format file is generated. Next, the generated XML
 111 format files and images are converted into TFRecord format files. Finally, the pre-trained model is read and the
 112 TFRecord format file is used for model training, resulting in the desired SSD model [16-18].

113 The training process of the Faster-RCNN model is shown in Figure 4:

114

115 **Figure 4** The training process of the Faster-RCNN model

116 For the Faster-RCNN model trained to identify the readings in the effective reading area, the effective reading
 117 area is firstly processed in grayscale, and then the brightness is adjusted, which can solve the problem that some
 118 images are too bright or too dark, and reduce the complexity of identifying the readings in the effective reading area.
 119 Secondly, LabelImg software is also used to label the numbers in the area, generate an xml format file, and convert it
 120 into a TFRecord format file. Finally, the model is trained to obtain the desired Faster-RCNN model [19-21]. The
 121 specific training steps for the two models are shown in Figure 5:

122

123 **Figure 5** The training steps for the models

124

125 2.3 Analysis of measurement data

126 The Faster-RCNN model and the SSD model are used to collect the electricity metering information of the total
 127 meter and sub-meters according to the pre-set time, and after the collection and summary, the user's electricity
 128 consumption information is transmitted to the master station, and the electricity consumption data is automatically
 129 copied and collected. The obtained measurement data is preprocessed, and then the estimation model and solution
 130 method are established through the preprocessed data. The estimation accuracy is checked, and finally, the purpose of
 131 online verification and business assistant decision-making is realized [22,23]. The specific process is shown in Figure
 132 6:

133

134

Figure 6 The process of scheme

135 The time series of original measurement data is preprocessed by the improved fuzzy C-means clustering
 136 technology, and the measurement data under light load conditions is excluded as the input variable of the online remote
 137 verification model [24]. Among them, the specific steps of preprocessing time series of the original measurement data
 138 based on the improved fuzzy C-means clustering are as follows:

139 Step 1: Determine the weighting index w and the iteration termination parameter ϵ according to the ratio of the
 140 increment of the electricity meter reading and the range of the electricity meter less than 0.1.

141 Step 2: Determine the number of clusters and cluster centers, sequentially select measurement data samples and
 142 substitute them into the hill-climbing function, as shown in the following equation (1):

$$143 \hat{M}^1(x_r) = \sum_{j=1}^n e^{-\alpha \|x_j - x_r\|^2} \quad (1)$$

144 In equation (1), x_j is the j th sample, and n is the total number of samples. x_r is the r th sample, which is the cluster
 145 center. $\hat{M}^1(x_r)$ is the hill-climbing function when the r th sample is taken as the cluster center, α is a positive number.

146 If $x_r = x_1^*$, where x_1^* is a sample in the sample set, get the first hill-climbing function to get the maximum value
 147 $\hat{M}_{max}^1 = \max(\hat{M}^1(x_1^*))$, x_1^* can be taken as the first cluster center [25]. When looking for other cluster centers, to
 148 eliminate the influence of x_1^* , the revised t th hill-climbing function is shown in the following equation (2):

$$149 \hat{M}^t(x_r) = \hat{M}^{t-1}(x_r) - \hat{M}_{max}^{t-1} \sum_{j=1}^n e^{-\beta \|x_j - x_{t-1}\|^2} \quad (2)$$

150 In equation (2), $\hat{M}^t(x_r)$ is the new hill-climbing function, $\hat{M}^{t-1}(x_r)$ is the hill-climbing function of the previous
 151 step, and \hat{M}_{max}^{t-1} is the maximum value of the hill-climbing function of the previous step. The process of finding cluster
 152 centers ends when $\hat{M}_{max}^t / \hat{M}_{max}^1 \leq \delta$, where δ is the convergence coefficient of the classification, which can be 0.001
 153 [26]. The total number of iterative clustering before judging convergence is the classification number c of fuzzy
 154 clustering. In each clustering process, the sample with the largest value of the hill-climbing function is x_t^* .

155 Step 3: The membership matrix is calculated, as shown in equation (3):

$$156 \quad \begin{cases} x_r = \frac{\sum_{j=1}^n (u_{rj})^w x_j}{\sum_{j=1}^n (u_{rj})^w} (1 \leq r \leq c) \\ u_{rj} = \left[\sum_{k=1}^c \left(\frac{\|x_j - x_r\|}{\|x_j - x_k\|} \right)^{2/(w-1)} \right]^{-1} (1 \leq r \leq c, 1 \leq j \leq n) \end{cases} \quad (3)$$

157 In equation (3), u_{rj} represents the membership degree of the j th sample with respect to the r th cluster center, w
 158 is the weighting index, and the value range is $[1, +\infty)$, and the value of w determines the fuzzyness of the final
 159 clustering effect. This method is taken as 1.8.

160 Step 4: The objective function is calculated, which is the weighted sum of squares of distances from each sample
 161 to all cluster centers, as shown in the following equation (4):

$$162 \quad J_w(\mathbf{U}, \mathbf{V}) = \sum_{j=1}^n \sum_{r=1}^c u_{rj}^w \|x_j - x_r\|^2 \quad (4)$$

163 Taking equation (4) as the iterative equation, when the two iteration errors $\Delta J_w(\mathbf{U}, \mathbf{V})$ before and after the
 164 objective function are less than the termination parameter \mathcal{E} , the clustering ends. The light load condition has been
 165 eliminated from the time series of the original measurement data, and the data preprocessing is completed.

166 After the data is preprocessed, an equation for solving the meter error is established. The remaining measurement
 167 data are sorted in chronological order to form the total and sub-meter matrices of the measurement data respectively,
 168 which are used as input samples for the error solution of the LMRLSA [27]. Based on the law of energy conservation,
 169 in any measurement period, the reading of the total meter is equal to the sum of the true values of each user sub-meter
 170 plus the sum of the line losses in this period [28]. For any t th measurement period, the relationship between the total
 171 meter and the sub-meter readings is shown in the following equation (5):

$$172 \quad y_0(t) = \sum_{i=1}^m z_i(t)(1 + \xi_i(t)) + w_{\text{loss}}(t) \quad (5)$$

173 In equation (5), $y_0(t)$ is the reading increment of the total meter in the measurement period, $z_i(t)$ is the reading
 174 increment of the i th sub-meter in the measurement period, and $\xi_i(t)$ is the error of the i th sub-meter in the measurement
 175 period. $z_i(t)(1 + \xi_i(t))$ is the power value actually consumed by the i th sub-meter in the measurement period, and
 176 $w_{\text{loss}}(t)$ is the power consumption of all lines in the measurement period, m is the total number of all sub-meters. The
 177 Levenberg-Marquardt (LM) algorithm is used to optimize the multi-layer feedforward neural network model to
 178 calculate the line loss [29]. Then, $1 + \xi_i(t)$ in equation (5) is represented by $\theta_i(t)$, and a set of measurement data
 179 series is formed by each unit measurement period $z_i(t)$ and the solution obtained $y(t)$. The equation (5) is written in
 180 matrix form, and the following equation (6) is obtained:

$$181 \quad \begin{cases} y(t) = \mathbf{Z}(t)\hat{\boldsymbol{\theta}}(t) \\ \hat{\boldsymbol{\zeta}}(t) = \hat{\boldsymbol{\theta}}(t) - \mathbf{I} \end{cases} \quad (6)$$

182 In equation (6), $\mathbf{Z}(t) = [z_1(t), z_2(t), \dots, z_m(t)]$ represents the measurement data matrix of each user's sub-meter
 183 in t th periods; $\hat{\boldsymbol{\theta}}(t) = [\theta_1(t), \theta_2(t), \dots, \theta_m(t)]^T$ refers to the error parameter matrix to be estimated by each user's sub-
 184 meter in the t th measurement period, and $\theta_i(t)$ denotes the operating error parameter of the i th meter to be found in
 185 the t th measurement period. $\hat{\boldsymbol{\zeta}}(t) = [\hat{\zeta}_1(t), \hat{\zeta}_2(t), \dots, \hat{\zeta}_m(t)]^T$ is the remote estimated value of the operating error of the
 186 electricity meter in the t th measurement period. After the equation is established, the operation error of the electricity
 187 meter is estimated through the LMRLSA. Specific steps are as follows:

188 Step 1: The initial value $\hat{\boldsymbol{\theta}}(0,0)$ and $\mathbf{P}(0,0) = \alpha \mathbf{I}$ are selected, where each element of $\hat{\boldsymbol{\theta}}(0,0)$ is 0 or a smaller
 189 number, $\mathbf{P}(0,0) = \alpha \mathbf{I}$, α is a large enough positive number, usually between 10^5 and 10^{10} , and \mathbf{I} is the unit matrix. L
 190 represents the memory length, and T refers to the latest measurement period. Compare T and L . If $T \leq L$, go to Step 2;
 191 if $T > L$, go to Step 3.

192 Step 2: When $T \leq L$, the ordinary Recursive Least Squares (RLS) algorithm is used to obtain the initial parameter
 193 estimate $\hat{\boldsymbol{\theta}}(0, L-1)$, its corresponding $\mathbf{P}(0, L-1)$ and the gain matrix $\mathbf{K}(0, L-1)$, and use it as the initial quantity of
 194 the LMRLSA. The specific process is as follows:

195 a. After the previous t measurements, the matrix equation can be obtained as shown in equation (7):

$$196 \quad \hat{\boldsymbol{\theta}}(t) = (\mathbf{Z}(t)^T \mathbf{Z}(t))^{-1} \mathbf{Z}(t)^T \mathbf{Y}(t) \quad (7)$$

197 In equation (7), $\mathbf{Z}(t) = \begin{bmatrix} z_1(1) & z_2(1) & \dots & z_m(1) \\ z_1(2) & z_2(2) & \dots & z_m(2) \\ \vdots & \vdots & \ddots & \vdots \\ z_1(t) & z_2(t) & \dots & z_m(t) \end{bmatrix}$ is the sub-meter matrix, $\mathbf{Y}(t) = \begin{bmatrix} y(1) \\ y(2) \\ \vdots \\ y(t) \end{bmatrix}$ is the total meter

198 matrix. It is assumed that $\hat{\boldsymbol{\theta}}(t-1)$ has been calculated in the $t-1$ recursion. Before the t th recursion, the time series

199 of the new total and sub-meter measurement data collected are respectively $y(t)$ and $\mathbf{Z}(t) = [z_1(t), z_2(t), \dots, z_m(t)]$.
 200 All the measurement data of each user sub-meter measured in the previous t times are represented by \mathbf{Z}_t , and all the
 201 measurement data of the total meter measured in the previous t times are represented by \mathbf{Y}_t . For the previous $t-1$
 202 measurements, they are represented by \mathbf{Z}_{t-1} , \mathbf{Y}_{t-1} respectively. Based on the measurement data collected in the
 203 previous $t-1$ measurement and the previous t measurement, the estimation result of the meter error parameter is shown
 204 in the following equation (8):

$$205 \quad \begin{cases} \hat{\boldsymbol{\theta}}(t-1) = (\mathbf{Z}_{t-1}^T \mathbf{Z}_{t-1})^{-1} \mathbf{Z}_{t-1}^T \mathbf{Y}_{t-1} \\ \hat{\boldsymbol{\theta}}(t) = (\mathbf{Z}_t^T \mathbf{Z}_t)^{-1} \mathbf{Z}_t^T \mathbf{Y}_t \end{cases} \quad (8)$$

206 b. The inverse $\mathbf{P}(t)$ of the covariance matrix of the measurement data is shown in equation (9):

$$207 \quad \begin{aligned} \mathbf{P}(t) &= (\mathbf{Z}(t)^T \mathbf{Z}(t))^{-1} \\ &= \left(\begin{bmatrix} \mathbf{Z}_{t-1}^T & \mathbf{Z}^T(t) \end{bmatrix} \begin{bmatrix} \mathbf{Z}_{t-1} \\ \mathbf{Z}(t) \end{bmatrix} \right)^{-1} \\ &= (\mathbf{Z}_{t-1}^T \mathbf{Z}_{t-1} + \mathbf{Z}^T(t) \mathbf{Z}(t))^{-1} \\ &= [\mathbf{P}^{-1}(t-1) + \mathbf{Z}^T(t) \mathbf{Z}(t)]^{-1} \\ &= \left[\mathbf{I} - \frac{\mathbf{P}(t-1) \mathbf{Z}^T(t) \mathbf{Z}(t)}{1 + \mathbf{Z}(t) \mathbf{P}(t-1) \mathbf{Z}^T(t)} \right] \mathbf{P}(t-1) \end{aligned} \quad (9)$$

208 c. The estimated value of the error parameter of each user's sub-meter is expressed as $\hat{\boldsymbol{\theta}}(t)$, and its calculation is
 209 shown in the following equation (10):

$$210 \quad \begin{aligned} \hat{\boldsymbol{\theta}}(t) &= (\mathbf{Z}_t^T \mathbf{Z}_t)^{-1} \mathbf{Z}_t^T \mathbf{Y}_t \\ &= \mathbf{P}(t) \begin{bmatrix} \mathbf{Z}_{t-1}^T & \mathbf{Z}^T(t) \end{bmatrix} \begin{bmatrix} \mathbf{Y}_{t-1} \\ y(t) \end{bmatrix} \\ &= \mathbf{P}(t) \begin{bmatrix} \mathbf{Z}_{t-1}^T \mathbf{Y}_{t-1} + \mathbf{Z}^T(t) y(t) \end{bmatrix} \\ &= \mathbf{P}(t) [\mathbf{P}^{-1}(t-1) \hat{\boldsymbol{\theta}}(t-1) + \mathbf{Z}^T(t) y(t)] \\ &= \mathbf{P}(t) \{ [\mathbf{P}^{-1}(t-1) - \mathbf{Z}^T(t) \mathbf{Z}(t)] \hat{\boldsymbol{\theta}}(t-1) + \mathbf{Z}^T(t) y(t) \} \\ &= \hat{\boldsymbol{\theta}}(t-1) + \mathbf{P}(t) \mathbf{Z}^T(t) [y(t) - \mathbf{Z}(t) \hat{\boldsymbol{\theta}}(t-1)] \end{aligned} \quad (10)$$

211 d. The defined gain matrix is expressed as $\mathbf{K}(t)$, as shown in the following equation (11):

$$212 \quad \mathbf{K}(t) = \frac{\mathbf{P}(t-1) \mathbf{Z}^T(t)}{1 + \mathbf{Z}(t) \mathbf{P}(t-1) \mathbf{Z}^T(t)} \quad (11)$$

213 e. Combined with equations (8) to (11), when $T \leq L$, the error check of the smart meter is shown in the following
 214 equation (12):

$$215 \quad \begin{cases} \mathbf{P}(t) = \mathbf{P}(t-1) [\mathbf{I} - \mathbf{K}(t-1) \mathbf{Z}(t)] \\ \hat{\boldsymbol{\theta}}(t) = \hat{\boldsymbol{\theta}}(t-1) + \mathbf{K}(t) [y(t) - \mathbf{Z}(t) \hat{\boldsymbol{\theta}}(t-1)] \end{cases} \quad (12)$$

216 Step 3: When $T > L$, the specific solution process of the LMRLSA module is directly entered, as follows:

217 a. When a new set of data of the latest measurement period T is added, based on the measurement data of the $L+1$
 218 group of smart meters from the $T-L$ th to the T th and the recursive calculation results of the previous $T-1$ times, the
 219 calculation process of the inverse matrix $\mathbf{P}(T-L, T)$ of the covariance of the measurement data is shown in equation
 220 (13):

$$221 \quad \begin{aligned} \mathbf{P}(T-L, T) &= (\mathbf{Z}(T-L, T)^T \mathbf{Z}(T-L, T))^{-1} \\ &= (\mathbf{Z}(T-L, T-1)^T \mathbf{Z}(T-L, T-1) + \mathbf{Z}^T(T) \mathbf{Z}(T))^{-1} \\ &= [\mathbf{P}^{-1}(T-L, T-1) + \mathbf{Z}^T(T) \mathbf{Z}(T)]^{-1} \\ &= \left[\mathbf{I} - \frac{\mathbf{P}(T-L, T-1) \mathbf{Z}^T(T) \mathbf{Z}(T)}{1 + \mathbf{Z}(T) \mathbf{P}(T-L, T-1) \mathbf{Z}^T(T)} \right] \mathbf{P}(T-L, T-1) \\ &= [\mathbf{I} - \mathbf{K}(T-L, T) \mathbf{Z}(T)] \mathbf{P}(T-L, T-1) \end{aligned} \quad (13)$$

222 In equation (13), the sub-meter reading matrix from $T-L$ th to T times is shown in equation (14):

$$223 \quad \mathbf{Z}(T-L, T) = \begin{bmatrix} \mathbf{Z}(T-L), \mathbf{Z}(T-L+1), \dots, \mathbf{Z}(T) \end{bmatrix}^T \\ = \begin{bmatrix} z_1(T-L) & z_2(T-L) & \dots & z_m(T-L) \\ z_1(T-L+1) & z_2(T-L+1) & \dots & z_m(T-L+1) \\ \vdots & \vdots & \ddots & \vdots \\ z_1(T) & z_2(T) & \dots & z_m(T) \end{bmatrix} \quad (14)$$

224 b. $\mathbf{K}(T-L, T)$ is defined as the gain matrix, as shown in equation (15):

$$225 \quad \mathbf{K}(T-L, T) = \frac{\mathbf{P}(T-L, T-1)\mathbf{Z}^T(T)}{1 + \mathbf{Z}(T)\mathbf{P}(T-L, T-1)\mathbf{Z}^T(T)} \quad (15)$$

226 c. The estimated value of the error parameter of the meter is calculated, as shown in equation (16):

$$227 \quad \begin{aligned} \hat{\boldsymbol{\theta}}(T-L, T) &= [\theta_1, \theta_2, \dots, \theta_m]^T \\ &= (\mathbf{Z}(T-L, T)^T \mathbf{Z}(T-L, T))^{-1} \mathbf{Z}(T-L, T)^T \mathbf{Y}(T-L, T) \\ &= \mathbf{P}(T-L, T) [\mathbf{Z}(T-L, T-1)^T \mathbf{Y}(T-L, T-1) + \mathbf{Z}^T(T) \mathbf{y}(T)] \\ &= \mathbf{P}(T-L, T) [\mathbf{P}(T-L, T-1)^{-1} \hat{\boldsymbol{\theta}}(T-L, T-1) + \mathbf{Z}^T(T) \mathbf{y}(T)] \\ &= \hat{\boldsymbol{\theta}}(T-L, T-1) + \mathbf{K}(T-L, T) \times [\mathbf{y}(T) - \mathbf{Z}(T) \hat{\boldsymbol{\theta}}(T-L, T-1)] \end{aligned} \quad (16)$$

228 Among them, the total meter reading matrix is expressed as: $\mathbf{Y}(T-L, T) = [\mathbf{y}(T-L), \mathbf{y}(T-L+1), \dots, \mathbf{y}(T)]^T$.

229 d. According to the above analysis, when a new set of T-th measurement data is added, the solution of the
230 LMRLSA is shown in the following equation (17):

$$231 \quad \begin{cases} \mathbf{K}(T-L, T) = \frac{\mathbf{P}(T-L, T-1)\mathbf{Z}^T(T)}{1 + \mathbf{Z}(T)\mathbf{P}(T-L, T-1)\mathbf{Z}^T(T)} \\ \mathbf{P}(T-L, T) = [\mathbf{I} - \mathbf{K}(T-L, T)\mathbf{Z}(T)]\mathbf{P}(T-L, T-1) \\ \hat{\boldsymbol{\theta}}(T-L, T) = \hat{\boldsymbol{\theta}}(T-L, T-1) + \mathbf{K}(T-L, T) \times [\mathbf{y}(T) - \mathbf{Z}(T)\hat{\boldsymbol{\theta}}(T-L, T-1)] \end{cases} \quad (17)$$

232 e. to keep the memory length L unchanged, the measurement data of a group of smart meters in the Tth is added,
233 and the measurement data of the T-Lth time needs to be removed. Based on the measurement data from the T-L+1th
234 to the L sets of T-th and the calculation result obtained by equation (17), the LMRLSA can be obtained when the
235 measurement data of the T-Lth is excluded. The solution of the LMRLSA is expressed as the following equation (18):

$$236 \quad \begin{cases} \mathbf{K}(T-L+1, T) = \frac{\mathbf{P}(T-L, T)\mathbf{Z}^T(T-L)}{1 - \mathbf{Z}(T-L)\mathbf{P}(T-L, T)\mathbf{Z}^T(T-L)} \\ \mathbf{P}(T-L+1, T) = [\mathbf{I} + \mathbf{K}(T-L+1, T)\mathbf{Z}(T-L)]\mathbf{P}(T-L, T) \\ \hat{\boldsymbol{\theta}}(T-L+1, T) = \hat{\boldsymbol{\theta}}(T-L, T) - \mathbf{K}(T-L+1, T) \times [\mathbf{y}(T-L) - \mathbf{Z}(T-L)\hat{\boldsymbol{\theta}}(T-L, T)] \end{cases} \quad (18)$$

237 Step 4: Based on the actual data, the calculation example analysis is carried out, and the online verification and
238 analysis of the estimation error result of the electricity meter is carried out, which includes the following contents:

- 239 a. Determine the ratio of the total number of electricity meters and the sample size;
- 240 b. Stratify according to the electricity consumption level of each user, thereby determining the number of smart
241 meter samples drawn from each layer;
- 242 c. The sum of the number of smart meters drawn from each layer should be equal to the sample size;
- 243 d. For the number that cannot be rounded, find its approximate value;
- 244 e. After the actual values of the extracted error parameters of smart meter are measured on-site by stratified
245 sampling, the Mean Absolute Percent Error (MAPE) and the Root Mean Square Error (RMSE) are used as judgments
246 basis. In the process of remote error verification of smart meter, the smaller the MAPE value and the RMSE value,
247 the higher the accuracy of the estimated error parameters [30]. If the total number of samples drawn on site is p, MAPE
248 and RMSE can be expressed by the following equations (19) and (20):

$$249 \quad MAPE = \frac{1}{p} \sum_{i=1}^p \frac{|\hat{\theta}_i - \theta_i|}{\theta_i} \times 100\% \quad (19)$$

$$250 \quad RMSE = \sqrt{\frac{1}{p} \sum_{i=1}^p (\hat{\theta}_i - \theta_i)^2} \quad (20)$$

251 In equations (19) and (20), θ_i is the actual error of the meter in the detected area, and $\hat{\theta}_i$ is the estimated value of
252 θ_i .

253 After that, a hierarchical processing mechanism for abnormal situations in low-voltage areas can be established.
254 Combined with the obtained results of the operation error of the smart meter, the degree of operation error of the
255 electricity meter, the proportion in the batch, the reason for the out-of-tolerance of the operation meter, the abnormal
256 level and other factors are analyzed to replace the status of smart meters, and perform services such as electricity theft
257 and electric leakage online detection [31,32].

259 3. Experimental Results and Analysis

261 3.1 Verification of image recognition effect

262 The TensorFlow Object Detection API provides the corresponding eval.py script to verify the trained model.
263 Running the script can verify the test set and generate the corresponding log file. Then, the log file is read through
264 TensorBoard and the verification effect of the model is displayed. The specific display effect is shown in Figure 7 and
265 Figure 8:

266
267
268
269
270
271
272
273
274
275
276
277
278
279
280
281
282
283
284
285
286
287
288
289
290
291
292
293
294
295
296
297
298
299
300
301
302
303
304
305
306
307
308
309
310
311
312
313
314
315
316
317
318
319
320
321

Figure 7 The SSD model detects the effective reading area of the electricity meter

Figure 8 The Faster-RCNN model identifies the specific readings of the electricity meter

The proposed step-by-step image recognition method is verified using the test data set, and the accuracy of recognition is calculated according to the recognition results. The specific verification scheme is shown in Figure 9.

Figure 9 Verification scheme

The verification scheme uses the Remote Procedure Call (RPC) image recognition interface implemented by the system for verification. Then, the recognition service of the image recognition terminal through the RPC interface is called to obtain the recognition reading results, and compare the recorded results with the correct readings. Finally, the recognition accuracy is counted. 528 electric meter images are used for testing. After testing and verification, the recognition accuracy is 98.49%.

3.2 Validation of remote verification methods

To verify the effectiveness of the proposed method, this experiment takes the actual electricity meter measurement data of a city in China from February to May 2021 as the object for analysis, and the frequency of the data collection is 15min. The research area contains 1 total meter and 195 user sub-meters. Through data preprocessing, no-load or light-load data is filtered out, and measurement data sets of different periods are obtained as analysis samples. The value of the memory length L is set to 1000, and the recursive estimation curve of the operation error of the smart meter solved by this method is shown in Figure 10:

Figure 10 The recursive estimation curve of the operation error of the electricity meter

Figure 10 denotes that there are 5 meters in the research area with extremely large errors, and the estimated error parameters of the remaining meters are all within the allowable range of normal errors. Taking any data in a measurement period, the estimated error value of the electricity meter in this period can be obtained, as shown in Figure 11:

Figure 11 The estimation error value of the electricity meter in a certain period

Figure 11 indicates that most of the error rates of the user sub-meters in the selected power distribution area are within the allowable range of normal errors. User sub-meters No. 48, 65, 112, 135, and 181 have errors out of tolerance. The error rate of the No. 48 meter is 4.2885%, the error rate of the No. 65 meter is 6.9741%, the error rate of the No. 112 meter is -14.1072%, the error rate of the No. 135 meter is 3.9381%, and the error rate of the No. 181 meter is 4.5189%. The user profile information obtained by the user information collection system can accurately locate the electricity customer information corresponding to the number of the smart meter whose error is out of tolerance, and collect the information of the smart meter. Based on the obtained potential out-of-tolerance meter information, through further analysis and verification, the specific reasons for the out-of-tolerance error of the smart meter are confirmed. For example, a positive error indicates that the electricity meter is aging and damaged, and a negative error indicates that the electricity meter is artificially destroyed, and there is electricity stealing behavior.

Based on the actual working conditions of the research area, the optimal value range of the memory length L is analyzed. The value of the memory length L in the proposed method is related to the frequency of the measurement data collected by the electricity meter in the area. The estimation error value of the electricity meter with different memory length L values is shown in Figure 12:

Figure 12 The estimation error value of the electricity meter with different memory length

Figure 12 refers that when $L=100$, the estimation error value of a normal smart meter seriously deviates from its actual error value, because the number of recursive estimation equations is in an underdetermined state when it is less than the number of error parameters to be estimated. The results cannot be applied. When $L=400$, the number of measurements is greater than the number of error parameters to be estimated, and the estimation error value begin to converge. However, the estimation error value of some normal smart meters are still in the out of tolerance range, and the estimation effect is not ideal. When $L=1000$, the estimation error value of each electricity meter is close to a certain value, and a more accurate estimation of the error parameters of the smart meter is obtained, and the estimation effect is ideal. When the value of L is large, although the error can also be estimated parameters, it takes a long time and reduces the efficiency of online analysis. Therefore, based on the actual working conditions of the research area, to ensure the accuracy of the estimated value and the real-time performance of the solution analysis, the recommended value of L ranges from 600 to 1200.

322 In this research, the line loss is considered in the calibration of the electricity meter, so if the calculation error of
323 the line loss is large, it will also affect the estimation result of the operation error of the electricity meter. When the
324 calculation errors of the line loss are 1%, 5%, 8%, and 10%, respectively, the comparison of the estimation error value
325 of each electricity meter is shown in Figure 13:

326
327 **Figure 13** The estimation error value of electricity meters under line losses of different errors

328 Figure 13 shows that when the error of the line loss calculation result is within 5%, it has little effect on finding
329 the out-of-tolerance electricity meter in the area, and the out-of-tolerance electricity meter can be accurately found,
330 and the effect is ideal. when the error of the line loss calculation result is about 8%, although the out-of-tolerance
331 meter can be found, the estimation error of the normal electricity meter is higher than its actual error value. There is a
332 situation of wrong detection, and the estimation effect is not good. When the error of the line loss calculation result is
333 more than 10%, the obtained out-of-tolerance meter has the situation of missed detection and wrong detection, and
334 the estimation effect is poor. The above analysis manifests that the line loss should be calculated as accurately as
335 possible to reduce the influence of the line loss on the estimation results of the operating error of the electricity meter.
336 Based on the current existing technical methods, it is necessary to ensure that the calculation accuracy of the line loss
337 is within 5%.

338 Data preprocessing is required to exclude data under light load conditions. The following analysis is made for
339 the light load condition. Based on the measurement data obtained by clustering under the light load condition, the
340 proposed algorithm is used to estimate the operation error of the smart meter. The results are shown in Figure 14:

341
342 **Figure 14** Estimation error value of electricity meter without excluding light load condition

343 Figure 14 means that when the measurement data under light load is used to remotely estimate the operating error
344 of the electricity meter, it is impossible to determine the out-of-tolerance meter, and most of the estimation error of
345 the electricity meter belong to the out-of-tolerance range. There are two main reasons: 1. The pulse generated by the
346 smart meter at light load is irregular, which will cause creeping phenomenon; 2. At light load, the proportion of
347 excitation loss and iron loss of the current transformer (CT) increases, which affects the error characteristic of the CT
348 and makes it enter the nonlinear region. At this time, there is no corresponding relationship between the error and the
349 load, and it is difficult to accurately compensate the error. Therefore, in the process of data preprocessing, the
350 measurement data at light load should be removed to the greatest extent to ensure the accuracy of the estimation error
351 of each user's smart meter and prevent over-checking.

352 353 4. Conclusion

354 With the continuous expansion of the scale of China's power grid, the number of electricity meters is also
355 increasing. The purpose is to simplify the verification method of the electricity meter and improve the work efficiency
356 while ensuring the calibration accuracy. Firstly, it is proposed to realize automatic meter reading through the Faster-
357 RCNN model and the SSD model, and the collected metering information is aggregated and sent to the master station.
358 Secondly, the original measurement data is preprocessed in the master station, and the measurement data under light
359 load conditions is excluded. Thirdly, the estimation error model and the solution equation of the electricity meter are
360 established based on the preprocessed data. The operation error of the electricity meter is estimated and the estimation
361 accuracy is checked by the LMRLSA. Combined with the remote verification results, the business assistant decision-
362 making is carried out. Finally, by the test of image recognition effect, it is verified that the image recognition system
363 based on the proposed Faster-RCNN model and the SSD model has an accuracy rate of 98.49%. Through the test of
364 remote verification effect, it is proved that the proposed algorithm can properly eliminate the influence of the old
365 measurement data on the error parameter estimation, improve the accuracy of the error parameter estimation value,
366 and ensure the real-time error estimation of the meter by adjusting the memory length. It can realize the function of
367 online monitoring whether there is electricity stealing or leakage by the recursive estimation curve. moreover, by
368 analyzing the influence of parameters on error results, it demonstrates that when the memory length ranges from 600
369 to 1200 and the line loss error is less than 5%, the accuracy of the electricity meter error estimation is most suitable.
370 Meanwhile, to avoid over-checking, the measurement data at light load should be removed as much as possible. Due
371 to limited energy, the proposed solution has not yet been completed for the development of the back-end, resulting in
372 very inconvenient data operations on the back-end. It will be improved in the future to improve the operation
373 experience. This research has certain reference significance for realizing intelligent remote online meter reading,
374 verification and management of electricity meters.

375 376 References

377

- 378 [1] Liu Y, Zhang J F, Yi Y, et al. The Development of Integrated Centralized Control Platform for Electricity Meter
379 Verification Device[J]. IOP Conference Series: Earth and Environmental Science, 2021, 766(1): 5.
- 380 [2] Dai Y, Xu D, Wang Q, et al. Research on Verification Error of Smart Electricity Meter based on Regression
381 Analysis[J]. Journal of Physics: Conference Series, 2020, 1486(6): 6.
- 382 [3] Liu F, Liang C, He Q. A Data-Based Approach for Smart Meter Online Calibration[J]. ACTA IMEKO, 2020,
383 9(2):32.
- 384 [4] Wang X, Wu D, Yuan R, et al. Dynamic test signal modelling and a Compressed Sensing based test for electric
385 energy meter errors[J]. Measurement, 2020, 164:107915.
- 386 [5] Tan Q, Wu P, Wei T, et al. Research on the Development Status, Strategic Choice and Business Model of China's
387 Charging Pile Industry[J]. Journal of Physics: Conference Series, 2020, 1637(1):6.
- 388 [6] Mansour R F, Escorcia-Gutierrez J, Gamarra M, et al. Intelligent video anomaly detection and classification using
389 faster RCNN with deep reinforcement learning model[J]. Image and Vision Computing, 2021(3):104229.
- 390 [7] Lv S, Liu K, Qiao Y, et al. Automatic defect detection based on improved Faster RCNN for substation
391 equipment[J]. Journal of Physics Conference Series, 2020, 1544:012157.
- 392 [8] Li C, Zhou P. Improved Faster RCNN Object Detection[J]. World Scientific Research Journal, 2020, 6(3):74-81.
- 393 [9] Yang B, Yang H, Zhang C, et al. SSD Model Selection Method Based on Machine Learning Algorithm[J]. Journal
394 of Physics Conference Series, 2021, 2005(1):012082.
- 395 [10] Zhang X, Gao Q, Pan D, et al. Research on Spatial Positioning System of Fruits to be Picked in Field Based on
396 Binocular Vision and SSD Model[J]. Journal of Physics Conference Series, 2021, 1748(4):042011.
- 397 [11] Zhang X, Xie H, Zhao Y, et al. A fast SSD model based on parameter reduction and dilated convolution[J].
398 Journal of Real-Time Image Processing, 2021, 18:2211-2224.
- 399 [12] Sindhvani N, Verma S, Bajaj T, et al. Comparative Analysis of Intelligent Driving and Safety Assistance Systems
400 Using YOLO and SSD Model of Deep Learning[J]. International Journal of Information System Modeling and
401 Design (IJISMD), 2021, 12(1): 131-146.
- 402 [13] Rani K, Rahim H A, Ong B T, et al. Mobile Green E-Waste Management Systems using IoT for Smart Campus[J].
403 Journal of Physics Conference Series, 2021, 1962(1):012056.
- 404 [14] Ghifari H G, Darlis D, Hartaman A. Pendeteksi Golongan Darah Manusia Berbasis Tensorflow menggunakan
405 ESP32-CAM[J]. ELKOMIKA Jurnal Teknik Energi Elektrik Teknik Telekomunikasi & Teknik Elektronika, 2021,
406 9(2):359.
- 407 [15] Sajeevan J P, Prajval P, Shwetha G P, et al. DNN Design for Object Detection in Airport Runway Operations[J].
408 International Journal of Advanced Science and Engineering, 2020, 6(12):223-225.
- 409 [16] Song Y, Wen Y. The Assisted Positioning Technology for High Speed Train Based on Deep Learning[J]. Applied
410 Sciences, 2020, 10(23):8625.
- 411 [17] Shi J, Chang Y, Xu C, et al. Real-time leak detection using an infrared camera and Faster R-CNN technique[J].
412 Computers & Chemical Engineering, 2020, 135:106780.
- 413 [18] Wang P, Wu J, Li X, et al. Fuzzy target detection algorithm based on improved SSD and transfer learning[J].
414 Journal of Intelligent and Fuzzy Systems, 2021(6):1-12.
- 415 [19] Xiong J, Zhu L, Ye L, et al. Attention aware cross faster RCNN model and simulation[J]. Wireless Networks,
416 2021, 198:1-13.
- 417 [20] Albahli S, Nawaz M, Javed A, et al. An improved faster-RCNN model for handwritten character recognition[J].
418 Arab. J. Sci. Eng., 2021, 46, 8509-8523.
- 419 [21] Li F, Xin J, Chen T, et al. An Automatic Detection Method of Bird's Nest on Transmission Line Tower Based on
420 Faster_RCNN[J]. IEEE Access, 2020, 8:164214-164221.
- 421 [22] Cui S, Gao Y, Yang Y, et al. Design and Research of Constant Magnetic Field Verification Device for Electric
422 Energy Meter[J]. IOP Conference Series: Earth and Environmental Science, 2021, 769(4):6.
- 423 [23] Kalinov D G, Rimlyand V I. Pre-Calibration of the Phase Interpolator of a Precision Time Interval Meter[J].
424 Measurement Techniques, 2020, 63(5):353-360.
- 425 [24] Zhao K, Dai Y, Jia Z, et al. General Fuzzy C-means Clustering Algorithm Using Minkowski Metric[J]. Signal
426 Processing, 2021, 188(C):108161.
- 427 [25] Kumar A, Sharma K, Sharma A. Genetically optimized Fuzzy C-means data clustering of IoMT-based biomarkers
428 for fast affective state recognition in intelligent edge analytics[J]. Applied Soft Computing, 2021, 109(4):107525.
- 429 [26] Nasir N, Samsudin R, Shabri A. Pre-processing Streamflow Data through Singular Spectrum Analysis with Fuzzy
430 C-Means Clustering[J]. IOP Conference Series: Materials Science and Engineering, 2020, 864(1):012085.
- 431 [27] Yadav S, Mohan R, Yadav P K. Task Allocation Model for Optimal System Cost Using Fuzzy C-Means
432 Clustering Technique in Distributed System[J]. Ingénierie des Systèmes D Information, 2020, 25(1):59-68.

- 433 [28] Bohnker J, Breuer K. Optimization of the recursive least squares algorithm for capacitive strain sensing[J].
434 Engineering Research Express, 2020, 2(4):046001.
- 435 [29] Mulashani A K, Shen C, Nkurl U B M, et al. Enhanced Group Method of Data Handling (GMDH) for
436 Permeability Prediction Based on the Modified Levenberg Marquardt Technique from Well Log Data[J]. Energy,
437 2021, 239(5):121915.
- 438 [30] Lv Z, Qiao L. Analysis of healthcare big data - ScienceDirect[J]. Future Generation Computer Systems, 2020,
439 109:103-110.
- 440 [31] Feizi A. Hierarchical detection of abnormal behaviors in video surveillance through modeling normal behaviors
441 based on AUC maximization[J]. Soft Computing, 2020, 24(6):10401-10413.
- 442 [32] Wan Z, Dong Y, Yu Z, et al. Semi-Supervised Support Vector Machine for Digital Twins Based Brain Image
443 Fusion[J]. Frontiers in Neuroscience, 2021, 15:705323.

Figure 1

The network structure of the Faster-RCNN model

The Faster-RCNN model is used to identify the specific readings of the dial image, but its running speed is relatively slow.

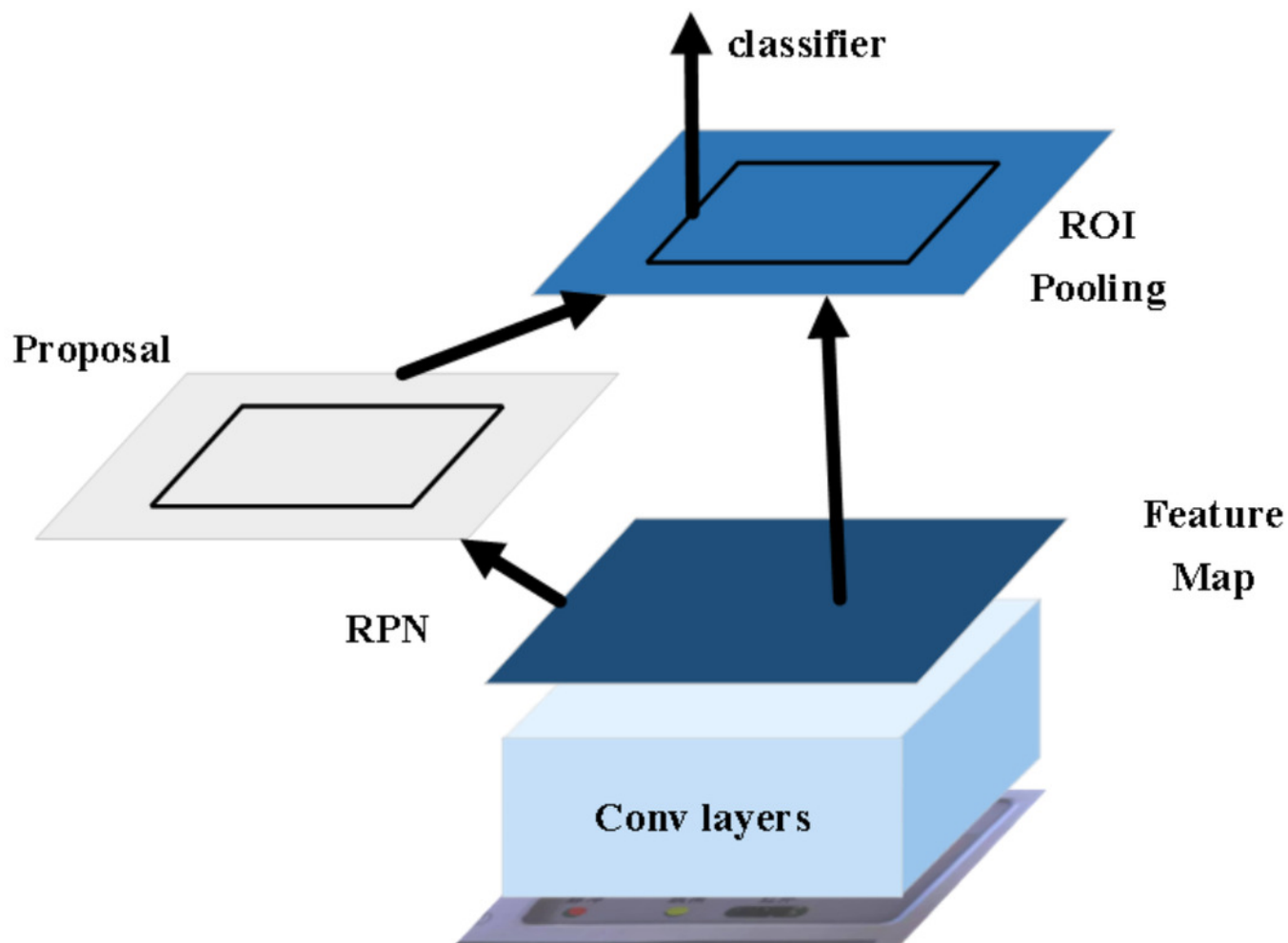


Figure 2

The network structure of the SSD model

The core of the SSD model is to predict the category score and offset of the candidate box. Simultaneously, candidate boxes of different sizes can be obtained by predicting on feature maps of different scales.

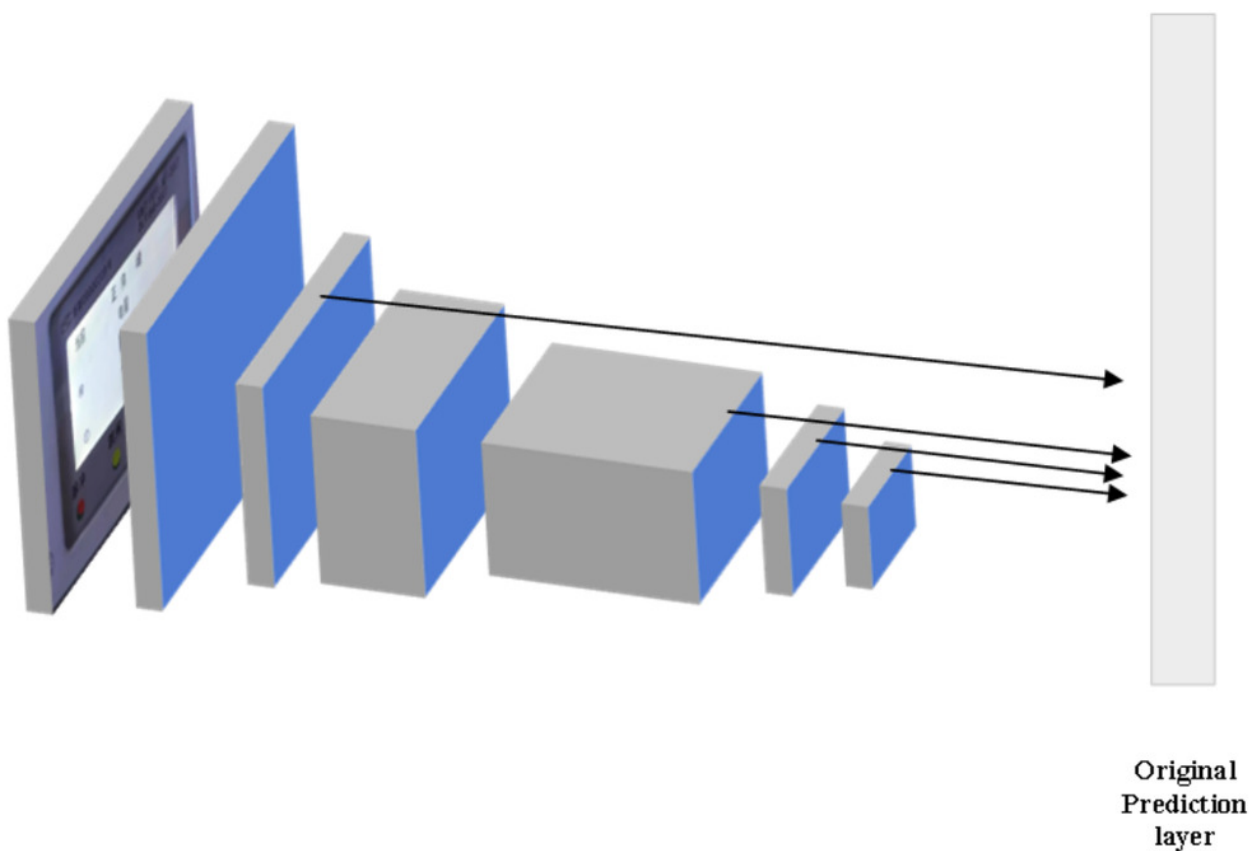


Figure 3

The specific training process of the SSD model

When training the SSD model, first, the input meter image is resized, the height of the image is uniformly set to 500px, and the width is scaled proportionally. Then, Labellmg software is used to label the effective reading area of the image screen, a training sample set is constructed, and an XML format file is generated. Next, the generated XML format files and images are converted into TFRecord format files. Finally, the pre-trained model is read and the TFRecord format file is used for model training, resulting in the desired SSD model.

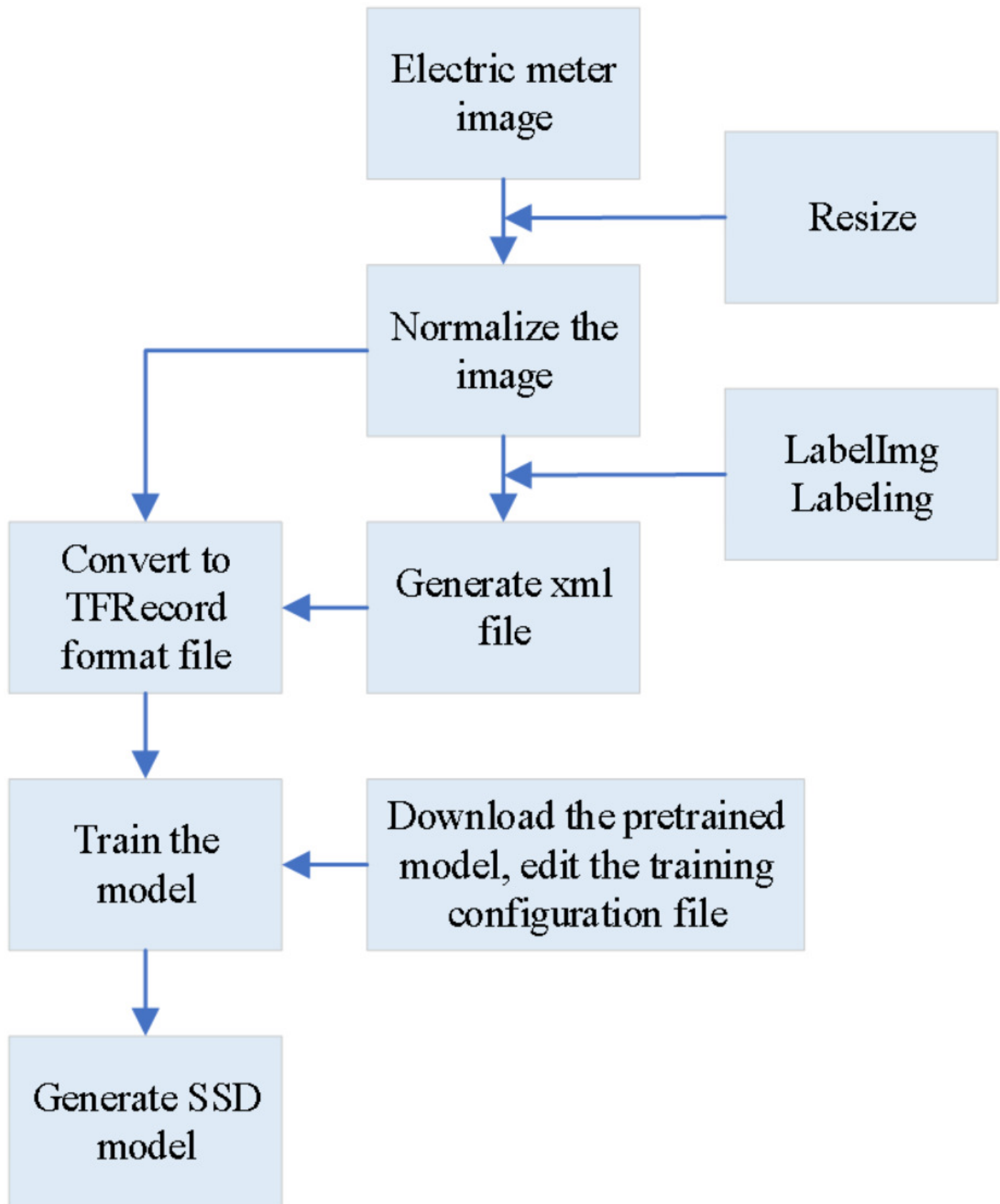


Figure 4

The training process of the Faster-RCNN model

For the Faster-RCNN model trained to identify the readings in the effective reading area, the effective reading area is firstly processed in grayscale, and then the brightness is adjusted, which can solve the problem that some images are too bright or too dark, and reduce the complexity of identifying the readings in the effective reading area. Secondly, Labelling software is also used to label the numbers in the area, generate an xml format file, and convert it into a TFRecord format file. Finally, the model is trained to obtain the desired Faster-RCNN model.

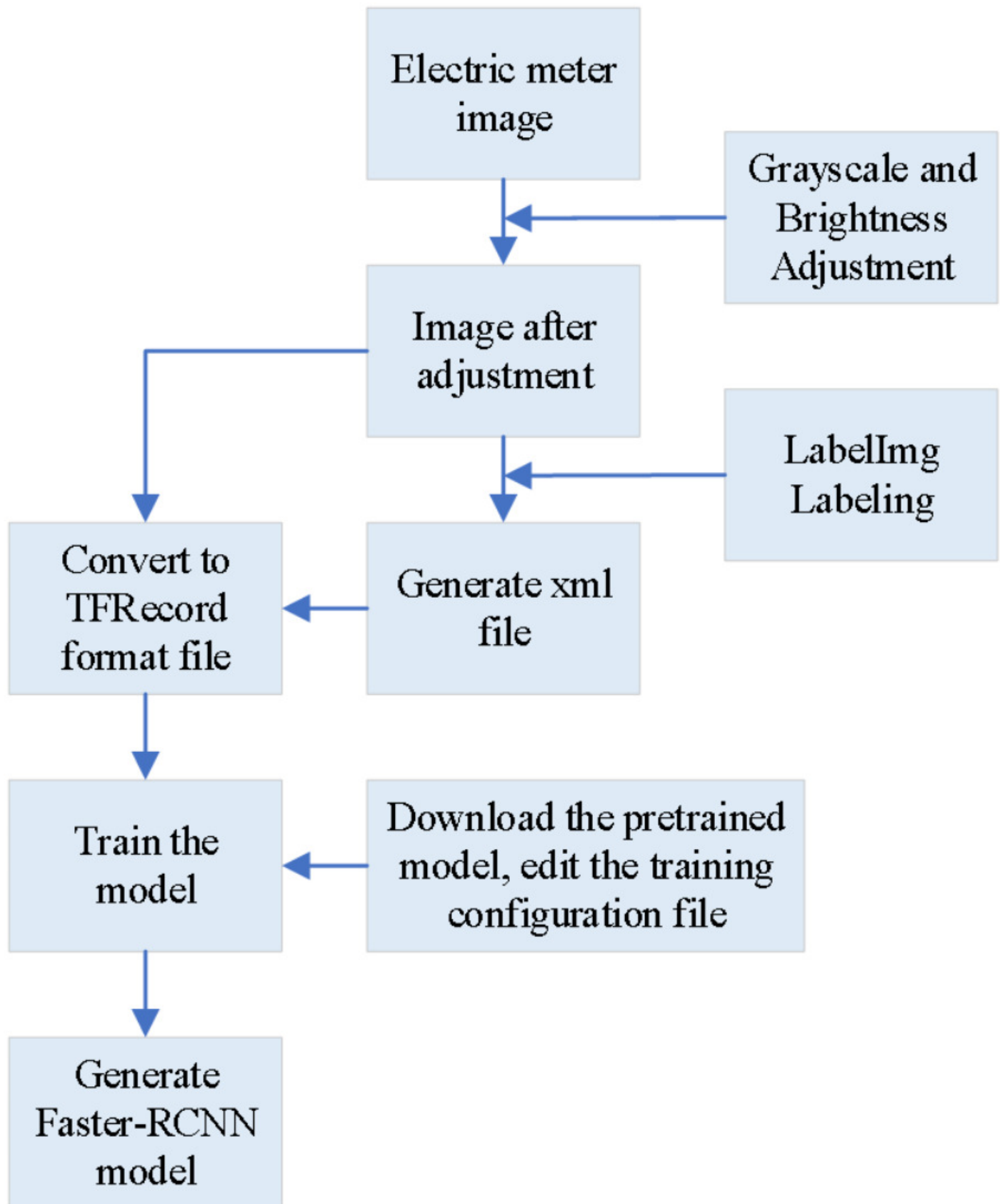


Figure 5

The training steps for the models

The specific training steps for the two models.

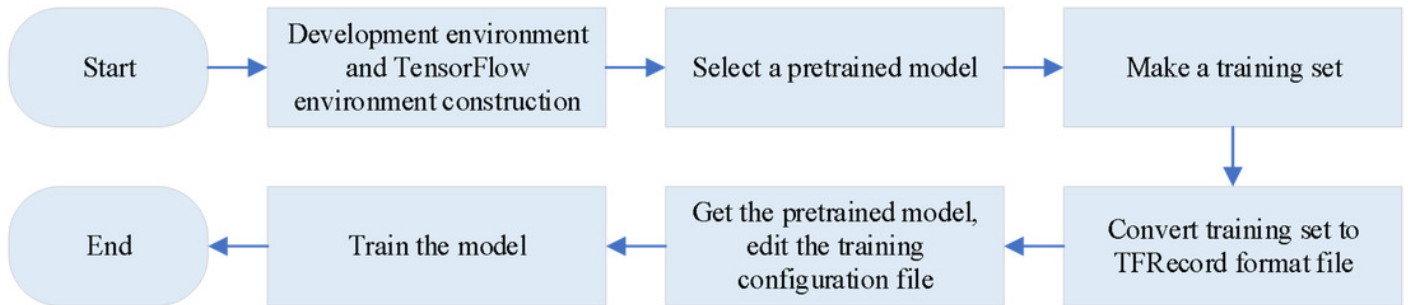


Figure 6

The process of scheme

The Faster-RCNN model and the SSD model are used to collect the electricity metering information of the total meter and sub-meters according to the pre-set time, and after the collection and summary, the user's electricity consumption information is transmitted to the master station, and the electricity consumption data is automatically copied and collected. The obtained measurement data is preprocessed, and then the estimation model and solution method are established through the preprocessed data. The estimation accuracy is checked, and finally, the purpose of online verification and business assistant decision-making is realized.

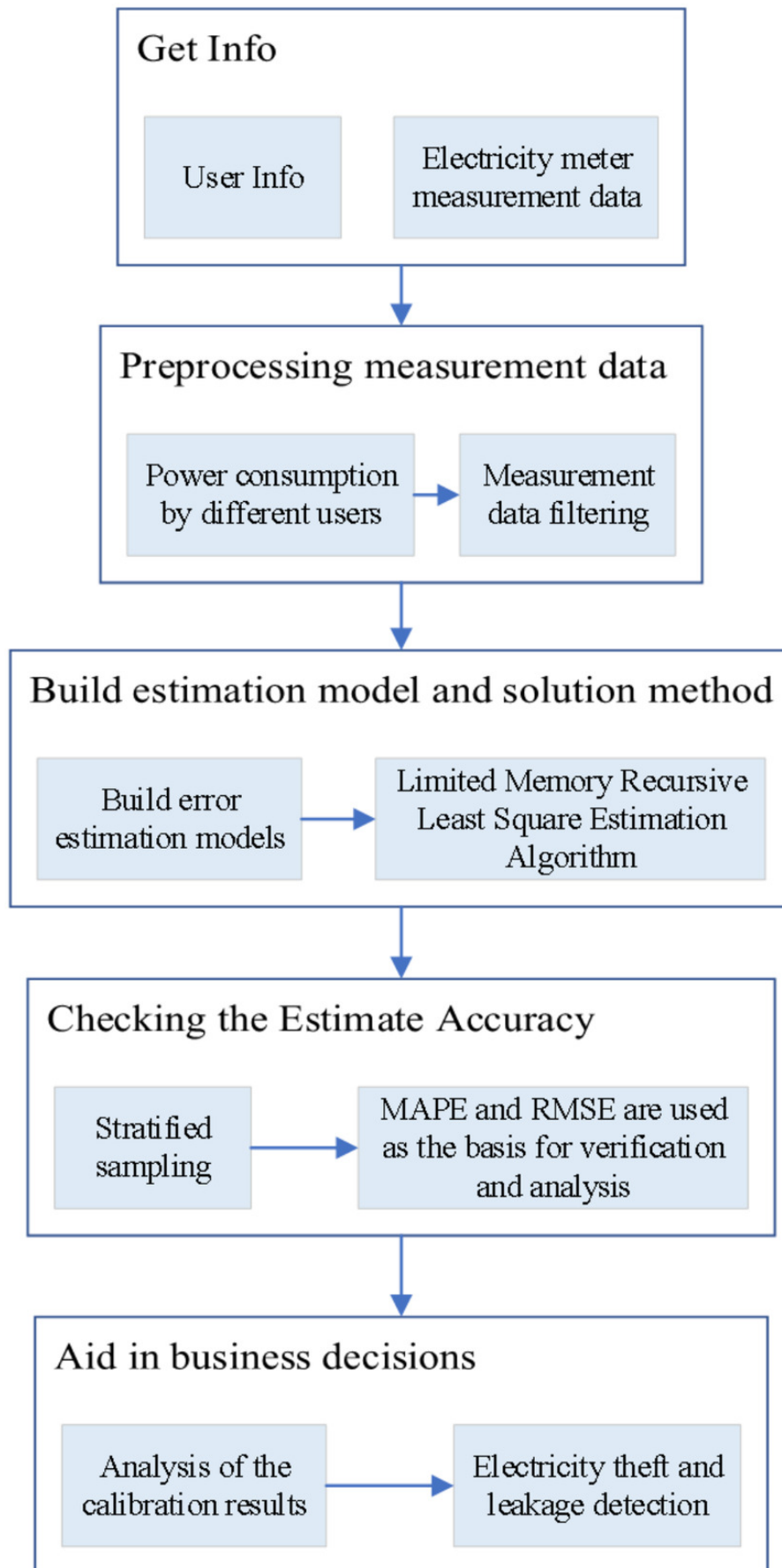


Figure 7

The SSD model detects the effective reading area of the electricity meter

The TensorFlow Object Detection API provides the corresponding eval.py script to verify the trained model. Running the script can verify the test set and generate the corresponding log file. Then, the log file is read through TensorBoard and the verification effect of the model is displayed.



Figure 8

The Faster-RCNN model identifies the specific readings of the electricity meter

The specific display effect



Figure 9

Verification scheme

The proposed step-by-step image recognition method is verified using the test data set, and the accuracy of recognition is calculated according to the recognition results.

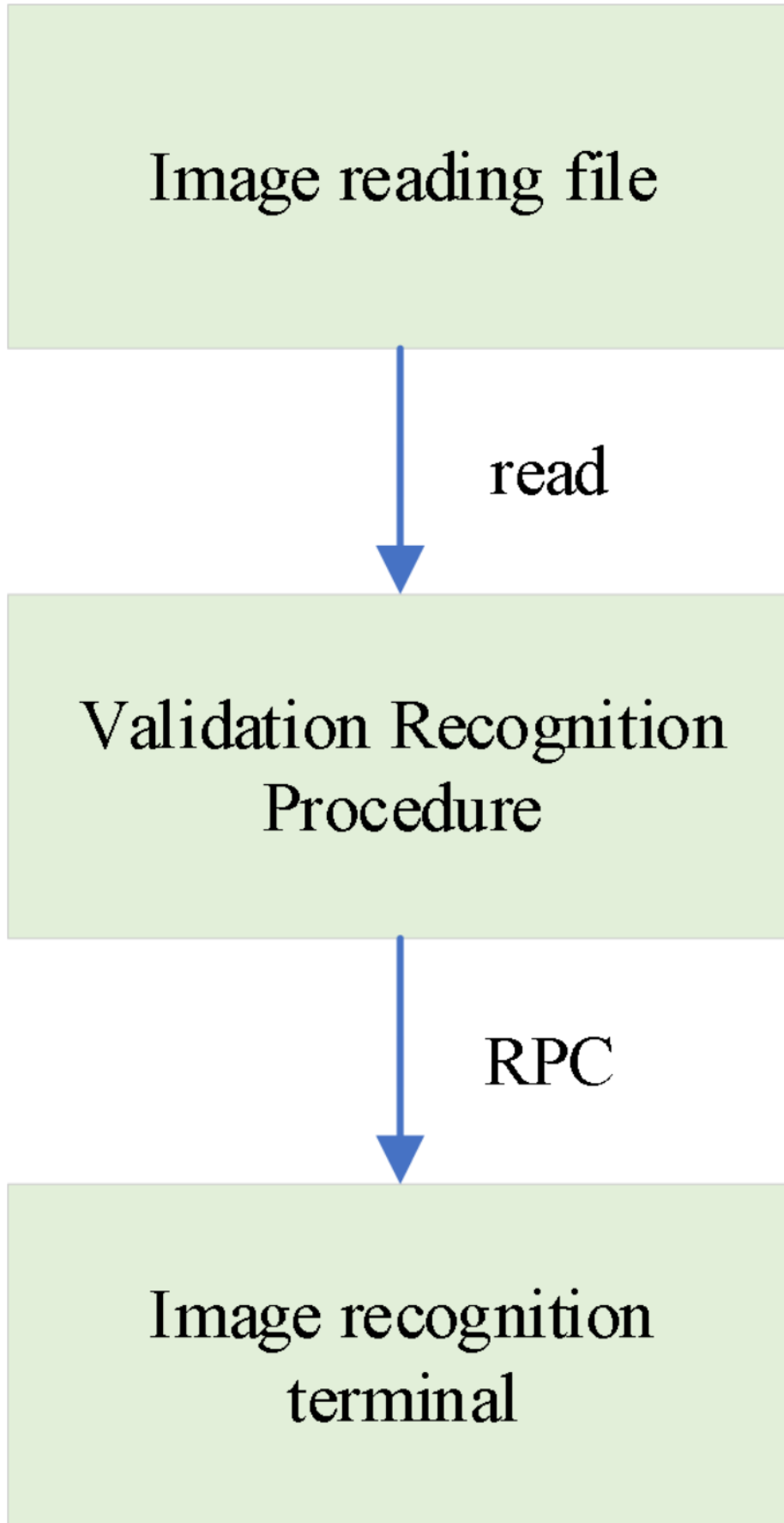


Figure 10

The recursive estimation curve of the operation error of the electricity meter

there are 5 meters in the research area with extremely large errors, and the estimated error parameters of the remaining meters are all within the allowable range of normal errors.

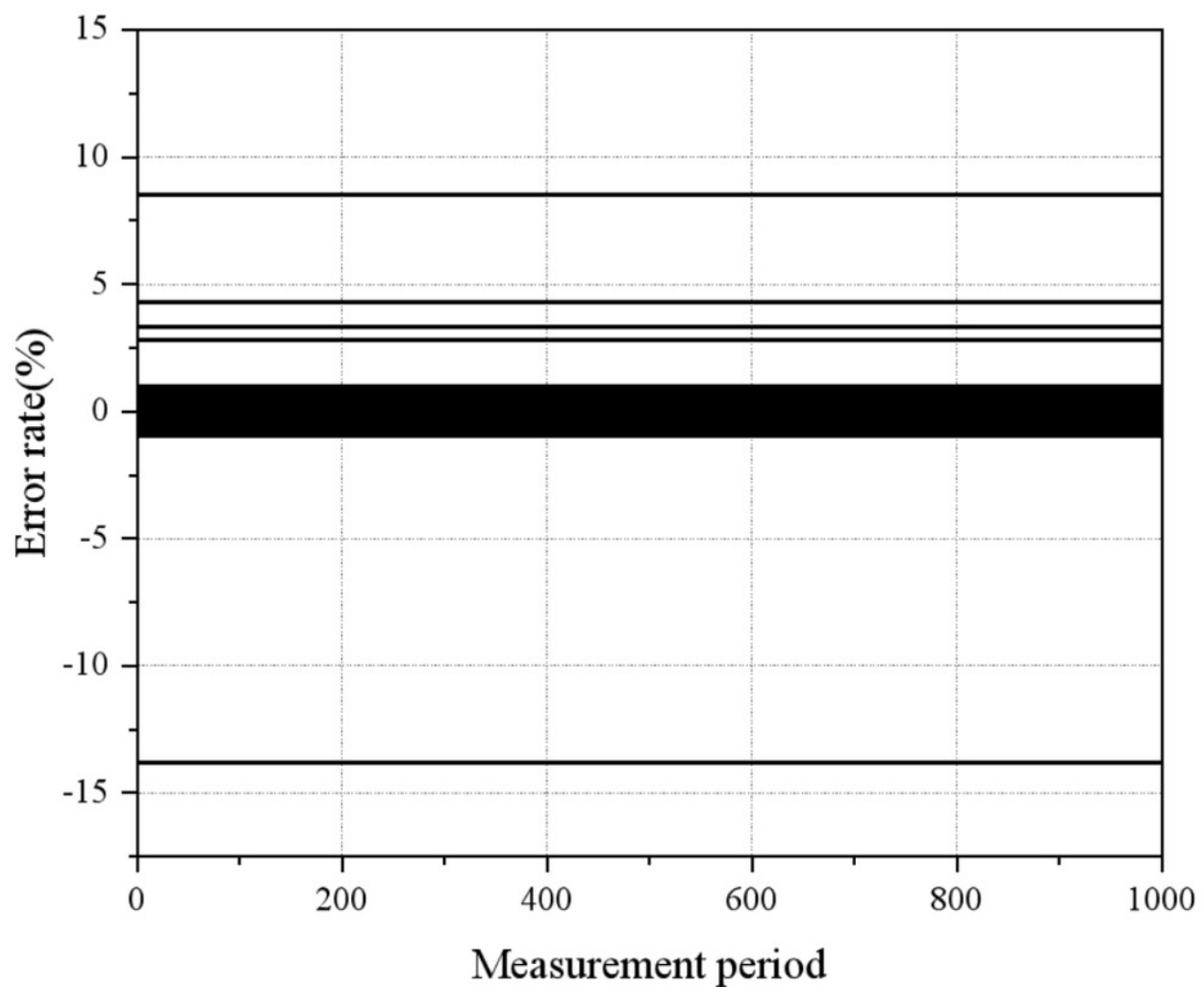


Figure 11

The estimation error value of the electricity meter in a certain period

Most of the error rates of the user sub-meters in the selected power distribution area are within the allowable range of normal errors. User sub-meters No. 48, 65, 112, 135, and 181 have errors out of tolerance.

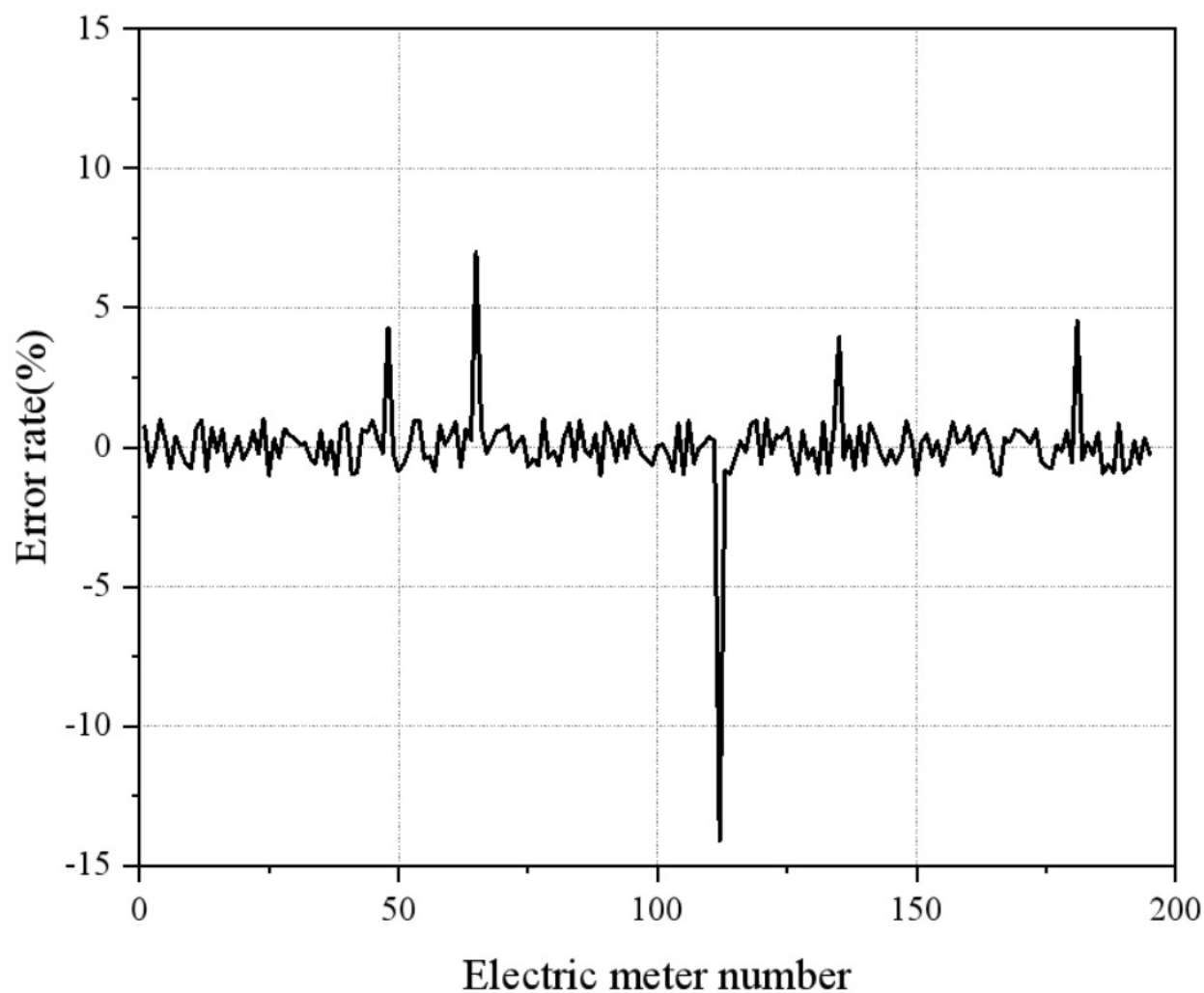


Figure 12

The estimation error value of the electricity meter with different memory length

When $L=100$, the estimation error value of a normal smart meter seriously deviates from its actual error value, because the number of recursive estimation equations is in an underdetermined state when it is less than the number of error parameters to be estimated. The results cannot be applied. When $L=400$, the number of measurements is greater than the number of error parameters to be estimated, and the estimation error value begin to converge. However, the estimation error value of some normal smart meters are still in the out of tolerance range, and the estimation effect is not ideal. When $L=1000$, the estimation error value of each electricity meter is close to a certain value, and a more accurate estimation of the error parameters of the smart meter is obtained, and the estimation effect is ideal. When the value of L is large, although the error can also be estimated parameters, it takes a long time and reduces the efficiency of online analysis. Therefore, based on the actual working conditions of the research area, to ensure the accuracy of the estimated value and the real-time performance of the solution analysis, the recommended value of L ranges from 600 to 1200.

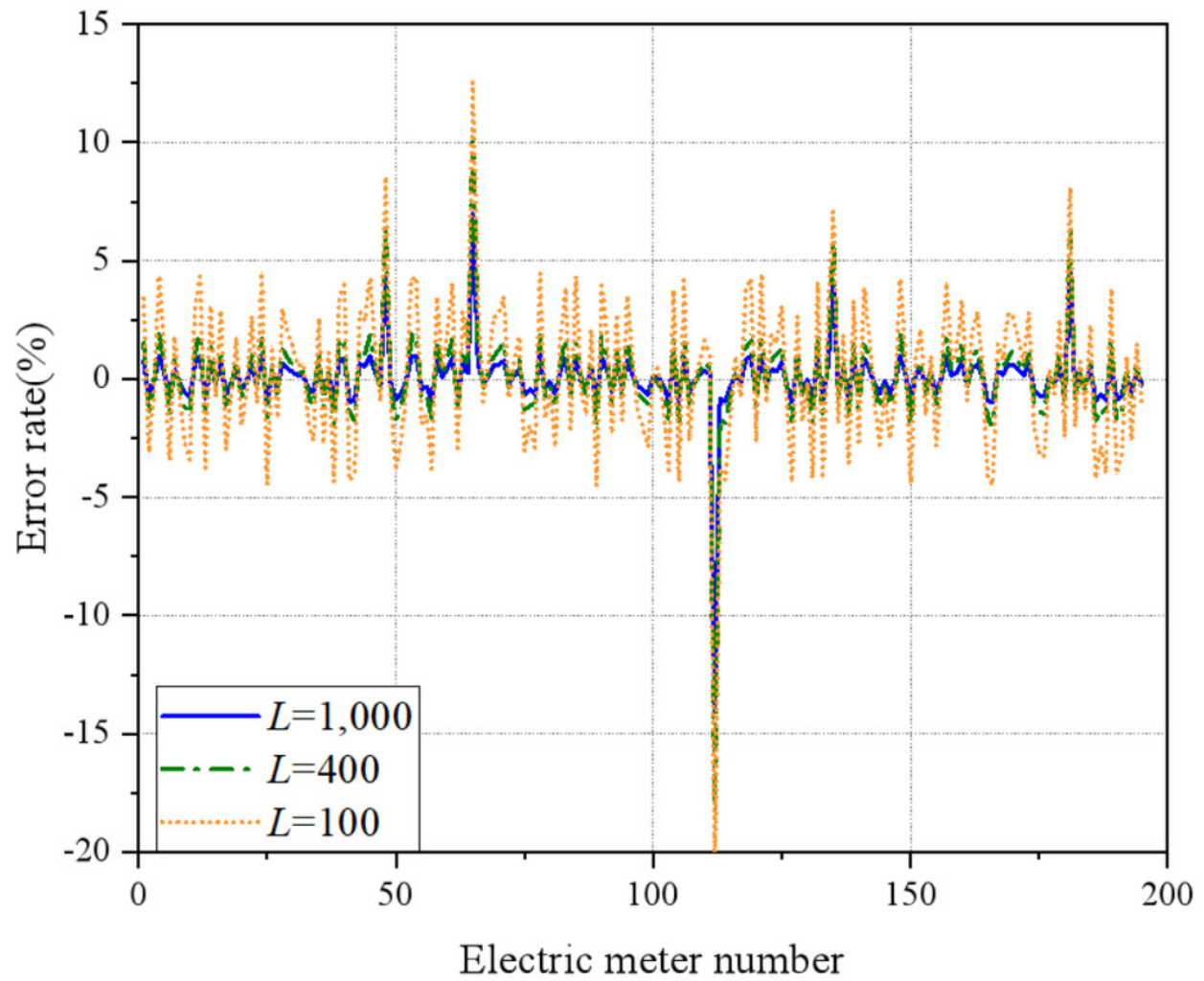


Figure 13

The estimation error value of electricity meters under line losses of different errors

When the error of the line loss calculation result is within 5%, it has little effect on finding the out-of-tolerance electricity meter in the area, and the out-of-tolerance electricity meter can be accurately found, and the effect is ideal. when the error of the line loss calculation result is about 8%, although the out-of-tolerance meter can be found, the estimation error of the normal electricity meter is higher than its actual error value. There is a situation of wrong detection, and the estimation effect is not good. When the error of the line loss calculation result is more than 10%, the obtained out-of-tolerance meter has the situation of missed detection and wrong detection, and the estimation effect is poor.

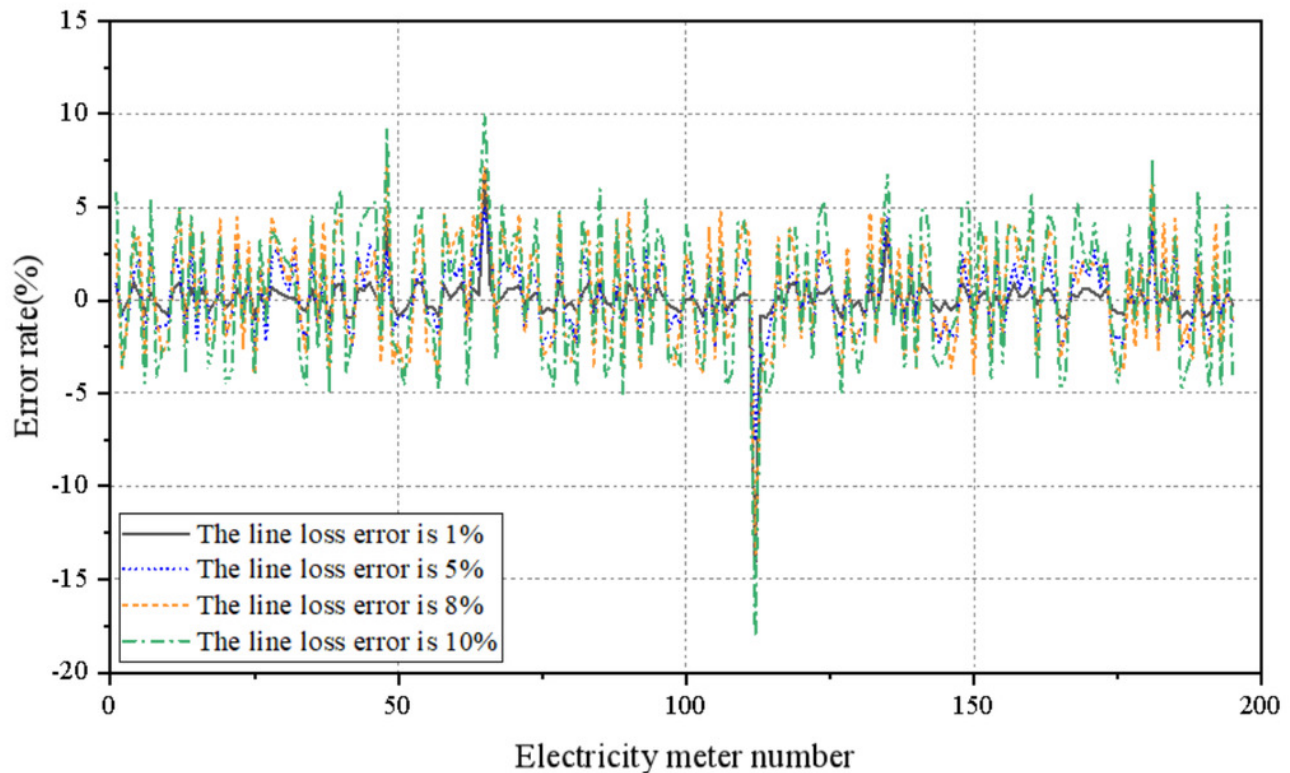


Figure 14

Estimation error value of electricity meter without excluding light load condition

When the measurement data under light load is used to remotely estimate the operating error of the electricity meter, it is impossible to determine the out-of-tolerance meter, and most of the estimation error of the electricity meter belong to the out-of-tolerance range.

